Svedberg Open
DISSEMINATION OF KNOWLEDGE

International Journal of Artificial Intelligence and Machine Learning

Publisher's Home Page: https://www.svedbergopen.com/

Research Paper Open Access

Dual-Band Thz MIMO Antenna Using Hybrid Defected Ground Structures, Machine Learning-Based Prediction, and Equivalent Circuit Modeling For Future Wireless Communications

Shiddanagouda.F.B[1,4], M.Lenin Kumar [2], Venkatapathi Pallam[3], S.Nagaveni[3], M.Khaleel Ullah Khan[4], K.Rambabu[4], Katapaka Yadaiah[4], Sai K Oruganti[1]

[1]Lincoln University College Selangor 47301 Malaysia
[2] Sri Muthukumaran Institute of Technology Chennai 600069 Tamil Nadu India
[3]CMR Institute of Technology Hyderabad 501401 Telangana India
[4]Vignan Institute of Technology and Science Hyderabad 508284 Telangana India
[1]siddu.kgp09@gmail.com

Abstract: Future wireless communication systems demand compact, high performance terahertz (THz) antennas, capable of supporting ultra-high data rates, large bandwidths and increased spectral efficiency. However, the wide bandwidth, high gain and low mutual coupling in compact THz multiple-input multiple-output (MIMO) antennas are still a great challenge. In this paper, a dual-band THz MIMO antenna is proposed designed on an 8-um thick Gallium Arsenide (GaAs) substrate using ANSYS HFSS. First, a rectangular microstrip patch antenna operating at 0.7 THz is designed, and then it is extended to a two-element MIMO configuration. To improve the antenna performance and miniaturization, the ground plane is incorporated with hybrid octagonal and hexagonal split-ring slot defected ground structures (DGSs). The proposed antenna provides dual-band operation at 0.55 THz and 0.73 THz with enhanced impedance bandwidth, improved gain and reduced mutual coupling. The MIMO characteristics are evaluated in terms of isolation, envelope correlation coefficient (ECC) and diversity gain (DG), showing excellent diversity operation for THz wireless communication applications. To mitigate the computational load due to repeated full-wave electromagnetic simulations, machine learning models are constructed with a dataset of 36,000 samples obtained from parametric HFSS simulations. Important antenna performance parameters are predicted using Decision Tree, Random Forest, K-Nearest Neighbors (KNN) and XGBoost regression algorithms. The Random Forest algorithm had the best prediction performance among the investigated models with R^2= 0.99986, MSE = 0.00675, RMSE = 0.08219, , and MAE = 0.04846. Furthermore, an equivalent lossy series RLC circuit model is developed in MATLAB for verification of the resonance characteristics and explanation of the antenna behavior at the circuit level. Moreover, the proposed design shows a virtual size reduction (VSR) of 21.26%, which means that the lower-band resonance at 0.55 THz is achieved with a compact physical structure. The results of the electromagnetic simulation and the predictions of the machine learning algorithm and the equivalent circuit model are in close agreement, thus validating the accuracy of the proposed methodology. The combined electromagnetic, machine learning and circuit-theoretic analysis demonstrates the effectiveness of the proposed antenna for compact THz MIMO systems and future wireless communication applications.

Keywords: Terahertz (THz) MIMO antenna, Defected Ground Structure (DGS), Machine Learning, Equivalent Circuit Model, Future Wireless Communications.

1. Introduction

The rapid expansion of Internet of Things (IoT) technologies has significantly increased the exposure of modern communication networks to security threats. With the growing use of smart surveillance systems, wearable devices, industrial sensors, and autonomous imaging platforms, IoT ecosystems are now generating enormous amounts of image-based data. The rapid growth of data-intensive applications such as ultra-highdefinition (UHD) video streaming, extended reality (XR), artificial intelligence (AI)-enabled services, autonomous driving, smart healthcare, industrial automation and massive Internet of Things (IoT) networks [1], [2] drives the evolution of next-generation wireless communication systems. These applications demand ultra-high data rates, ultra-low latency, high reliability and enhanced spectral efficiency to facilitate seamless connectivity among billions of devices. However, the conventional microwave and millimeter wave frequency bands are rapidly approaching their fundamental limits in terms of available bandwidth, spectral efficiency and network capacity [3]. This has caused the research focus to move towards higher frequency spectra in order to satisfy the growing demand for ultra-fast wireless connectivity.

The terahertz (THz) frequency band (0.1–10 THz) is proposed as a promising candidate for future wireless communication systems because of its extremely wide unused bandwidth, which can potentially achieve terabit-per-second data transmission and ultra-low latency communication [4], [5]. In addition to communication properties, THz waves have unique characteristics including non-ionizing radiation, high-resolution imaging, spectroscopic sensing and great potential in biomedical and security applications. Figure 1 summarizes the key features and advantages of THz communication systems, with the spectrum expansion, ultra-high capacity ability and compact device integration due to short wavelengths. However, THz propagation is limited by free-space path loss, molecular absorption and atmospheric attenuation, which restrict the communication range and reliability severely [6]. Therefore, dense small-cell deployment and super-efficient antenna systems are needed to fully exploit the THz spectrum. The short wavelength at THz frequency allows a large antenna miniaturization and the possibility to integrate multiple antenna elements in a small area, making multiple-input multiple-output (MIMO) technology very suitable for THz systems [7]. MIMO systems offer diversity gain to improve reliability and spatial multiplexing to improve 1000 times channel capacity. The major advantages of MIMO technology are summarized in Figure 2, including data rate, spectral efficiency, coverage and link reliability improvement. They also enable beamforming, which directs radiation toward desired users, improving signal strength while reducing interference and increasing energy efficiency. However, the compact MIMO arrangements with antenna elements placed in a close proximity experience a severe electromagnetic coupling, which causes impedance mismatch, reduced radiation efficiency, degradation in the isolation and deterioration in the performance [8]. Therefore, the design of THz MIMO antennas with compact size, wide bandwidth, high gain and low mutual coupling is still a great challenge.

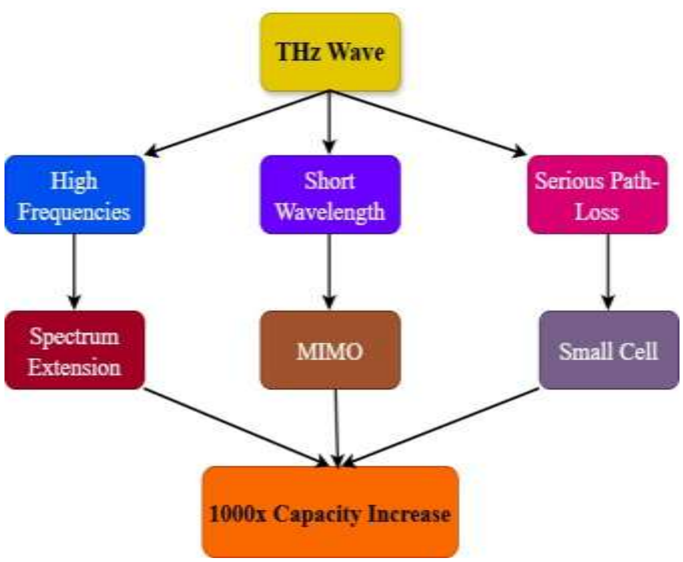

Fig 1: THz communication characteristics

Fig 2. Benifits of MIMO Antennas

To overcome these limitations, several techniques such as electromagnetic band-gap (EBG) structures, metamaterials, parasitic elements, neutralization lines, and defected ground structures (DGSs) have been investigated [9], [10]. Among these, DGS based approaches are popularly employed due to their ability to alter the ground current distribution, suppress the surface waves, improve the impedance matching, improve the isolation and also to facilitate the miniaturization of the antenna without significantly increasing the structural complexity. However, simultaneous dual-band operation, compactness, high gain, and strong isolation of THz MIMO antennas are challenging and need advanced design and optimization strategies. Design and optimization of THz antennas is often carried out with full-wave electromagnetic simulators like HFSS, which involve repetitive parametric sweeps and iterative optimization. With the complexity of antenna structures increasing, this traditional trial and error approach becomes computationally expensive and time consuming [11]. To overcome this limitation, artificial intelligence (AI)-based techniques, in particular machine learning (ML), have received a lot of attention recently in antenna engineering. Figure 3 depicts the relationships between AI, ML and DL, and the learning paradigms of supervised learning, unsupervised learning and reinforcement learning. The supervised learning algorithms such as decision trees, random forests, gradient boosting methods, K-nearest neighbors and neural networks are widely used for modeling the nonlinear relationship between antenna geometrical parameters and electromagnetic responses in antenna applications [12], [13]. Once trained, these surrogate models can quickly predict the performance of an antenna without having to repeatedly perform full wave simulations, thus significantly reducing the computational cost.

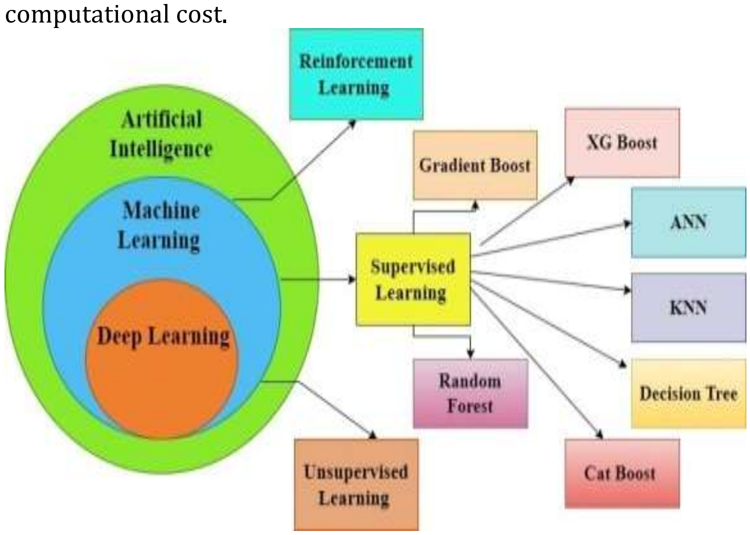

Fig 3. Hierarchy of AI, ML, DL with Learning Types

However, machine learning models, despite their predictive ability, often lack physical interpretability on the underlying electromagnetic resonance mechanisms. An alternative analytical approach to bridge this gap is an equivalent circuit model. The resonant behavior, impedance characteristics and frequency response of the antenna can be well represented by lumped circuit elements [14] for a lossy series RLC model. This circuit-like representation not only verifies the electromagnetic simulation and ML predictions but also offers a deeper physical insight into the operation mechanism of the antenna. Hence, combining full-wave simulation, machine learning prediction and equivalent circuit modeling provides a comprehensive and efficient antenna design framework.

The above challenges motivate the presented compact dual-band THz MIMO antenna with hybrid octagonal and hexagonal split-ring slot defected ground structures. The proposed design leads to miniaturized antennas, improved impedance bandwidth, enhanced gain and reduced mutual coupling. To speed up the design process, a machine learning based surrogate model is developed based on a dataset of 36000 samples generated by parametric HFSS simulation, which can accurately and quickly predict the antenna performance. Also, an equivalent lossy series RLC circuit model is developed in MATLAB to verify the resonance characteristics and to give physical interpretation of the proposed antenna structure. The good agreement between the electromagnetic simulation, machine learning prediction and equivalent circuit analysis results shows the effectiveness and accuracy of the proposed method to design compact THz MIMO antennas for future wireless communication systems.

2. Related Work

Recently, the research on THz antenna has been focused on improving the key performance parameters such as gain, radiation efficiency, impedance bandwidth and compactness. Sharma and Singh [6], Uddin et al. [8] and Mulakala et al. [9] have proposed compact THz antenna designs with enhanced impedance bandwidth and radiation characteristics. Like these, Sree Keerthana et al. [15], Bhavani et al. [16] and Armghan et al. [17] have reported broadband and high gain terahertz antennas for high frequency wireless applications. Although these contributions are representative for the progress in THz antenna design, most of the works are limited to the improvement of individual performance metrics. The open problem is to realize simultaneously a compact dual band high gain and wide impedance bandwidth antenna.

The THz MIMO antenna designs have also been investigated for the enhancement of the diversity performance and the channel capacity. Pant and Malviya [10] demonstrated a compact THz MIMO antenna with enhanced isolation and low envelope correlation coefficient (ECC). Alharbi and Sorathiya [11] proposed the THz MIMO antenna with reduced mutual coupling and better isolation. These works prove the effectiveness of MIMO techniques. Nevertheless, the majorities of the reported configurations are restricted to single-band operation or are mainly focused on improving the isolation. Compact dual band THz MIMO antennas with high gain, low ECC, mutual coupling reduction and high diversity performance are still relatively few.

Defected ground structures (DGSs) have been widely studied to enhance the antenna performances. DGS structures for the improvement of impedance matching and reduction of mutual coupling have been proposed by Kumar et al. [9], Mishra et al. [23] and Acharjee et al. [24] in the form of dumbbell-shaped and H-shaped geometries. U-shaped, circular and rectangular DGS configurations were studied by Zhang et al. [25], Li et al. [26] and Ahmed et al. [27] respectively to improve bandwidth and radiation performance. Furthermore, DGS structures based SRR and CSRR have been proved with better isolation and miniaturization performance by Chen et al. [28] and Wang et al. [29]. But most studies examine only one DGS geometry. Limited studies have dealt with hybrid DGS configurations with multiple geometric structures to simultaneously improve bandwidth, gain, isolation and miniaturization, particularly for THz MIMO antennas.

In this paper, explore the application of machine learning based antenna modeling to reduce the computational cost and improve the design efficiency. Biswas and Tiwari [30], Reddy et al. [31], Haque et al. [32], U-X et al. [33], Tomar and Kumari [34], Lahiri et al. [35], and Han et al. [36] proved that machine learning models are effective in prediction of antenna characteristics with parametric datasets and less simulation time than conventional optimization methods. However, most of the studies are limited to single antenna structure or limited datasets and the comparative evaluations using multiple regression algorithms for THz MIMO antenna prediction are not available.

The equivalent circuit modeling confirmed the antenna resonance behavior in an analytical manner. Lossy series RLC equivalent circuits were used to model antenna impedance characteristics, resonant behavior and quality factor by F Costa et al. [37], C A Balanis et al. [38], R Garg et al. [39], Hong et al. [40] and Deshmukh et al. [34]. These models give a good physical insight into the way the antenna works. They provide an alternative method of validating full-wave simulations. However, most of the existing works focus on the equivalent circuit modeling in isolation without integrating it with electromagnetic simulation and machine learning based prediction in a unified antenna design framework. The main limitation of the existing works according to the above review is the lack of a unified design approach for designing compact THz MIMO antenna structures with dual-band operation, high gain, wide impedance bandwidth, low mutual coupling and strong diversity performance. Furthermore, systematic study of hybrid defected ground structures for THz antenna miniaturization is still rare. Moreover, the current machine learning-based antenna studies are mostly limited to small data sets and one-model studies, which restrict the robust performance evaluation of complex antenna systems. Usually the equivalent circuit modeling is used as an isolated validation tool, and not as part of a comprehensive antenna analysis framework. These limitations motivate a unified framework integrating antenna design, machine learning, and equivalent circuit modeling for high-performance THz MIMO antenna systems.

3. Antenna Design Methodology

Figure 4 shows the full design methodology and the geometrical evolution of the suggested THz antenna.

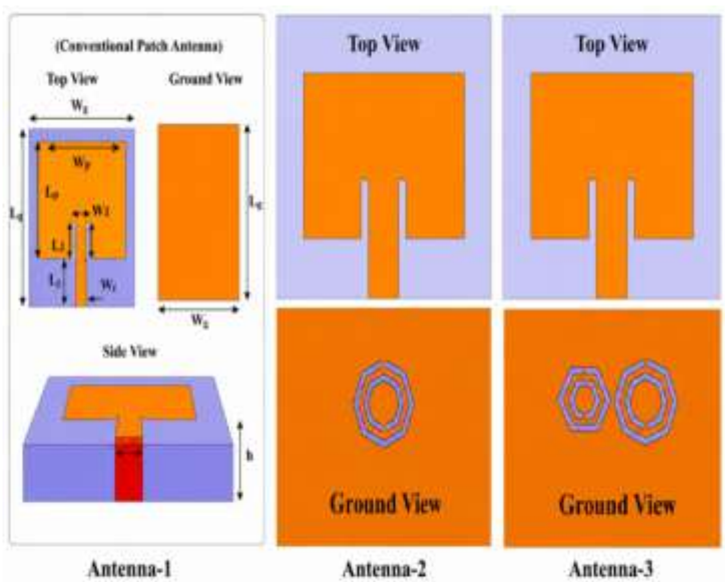

Fig 4. Hierarchy of AI, ML, DL with Learning Types

The design procedure begins with the choice of the target operating frequency and substrate material in accordance with the intended application. In this work a resonant frequency of 0.7THz and a substrate of Gallium Arsenide (GaAs) of thickness 0.8μm were selected. The dimensions of the antenna were calculated using standard design equations for a rectangular microstrip patch antenna based on the transmission-line model involving the speed of light (c), resonant frequency (fr), dielectric constant of the substrate (εr), effective dielectric constant (εeff) and the thickness of the substrate (h). The patch width (Wp) and patch length (Lp) were designed using equations (1)–(2) to get proper resonance, efficient radiation and 50-Ω impedance matching[38][39].

$$W_p = \frac{C}{2f_r}\sqrt{\frac{2}{\varepsilon_r + 1}} \qquad (1)$$

$$L_p = \frac{C}{2f_r\sqrt{\varepsilon_{eff}}} \qquad (2)$$

The dimensions of the ground plane are calculated by equations (3) and (4), [38][39] for efficient radiation and proper impedance matching. The calculated dimensions fed into electromagnetic simulator ANSYS HFSS.

$$L_s = L_p + 6h \qquad (3)$$

$$W_s = W_p + 6h \qquad (4)$$

The calculated dimensions were then implemented and optimized in ANSYS HFSS resulting in Antenna-1, the geometry of which is shown in top, ground and side views in Fig. 4. The antenna consists of a rectangular radiating patch, inset feed line, GaAs substrate and full ground plane. The dimensions are Ls=179.5µm, Ws = 211.5µm, Lp= 100µm, Wp = 148µm, L1 = 34µm, W1 = 7.5µm, Lf= 31.78µm, Wf = 23.5µm and h = 0.8µm. Antenna-1 is the reference structure, which resonates at 0.7THz with a return loss of approximately −35dB, bandwidth of 120GHz and peak gain of 5dB. An Octagonal Split-Ring Slot Defected Ground Structure (OSRSDGS) was etched in the ground plane below the radiating patch to create Antenna-2 for improving the electromagnetic performance. The enlarged geometry of the OSRSDGS is depicted in Figure 5 where the optimized dimensions obtained through HFSS parametric analysis are S1 = 30µm, S2 = 20µm, S3 = 7µm, H_w = 2µm and G = 2µm.

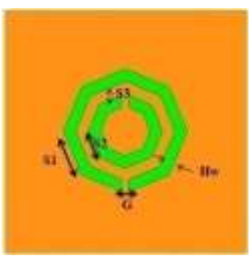

Fig 5. Geometry of OSRSDGS

The OSRSDGS functions as an equivalent LC resonator with the inductance being provided by the slot perimeter and the capacitance by the split gap that distorts the ground-current distribution, increases the effective electrical length, better the impedance matching and improves the radiation characteristics. This leads to the Antenna-2 with an improved return loss of about -40dB, bandwidth of 130GHz and peak gain of 5.45dB, with the resonance at 0.7THz. Antenna-3 is formed by using Hexagonal Split-Ring Slot Defected Ground Structure (HSRSDGS) along with OSRSDGS to improve antenna characteristics and add more resonant modes. The optimized dimensions of the HSRSDGS are S1 = 30µm, S2 = 20µm, S3 = 7µm, H_w = 2µm, and G = 2µm, and its enlarged geometry is shown in Figure 6.

Fig 6. Geometry of HSRSDGS

The HSRSDGS was placed at a distance of 0.02μm from the OSRSDGS to achieve the strong electromagnetic coupling between the two resonators. The coupling of the octagonal and hexagonal resonators causes mode splitting and excites more resonant modes due to their different electrical lengths and current distributions, which changes the antenna from a single-band to a dual-band structure. The performance evolution is also shown in Figures. 7-11. The simulated return-loss characteristics of Antenna-1, Antenna-2 and Antenna-3 are shown in Figure 7 which demonstrates the progressive improvement due to the introduction of DGS structures. Antenna-1 and Antenna-2 resonate at 0.7THz, while Antenna-3 operates in dual-band at 0.55THz and 0.73THz with return losses of around −43dB and −34dB and bandwidths of 47GHz and 44GHz, respectively.

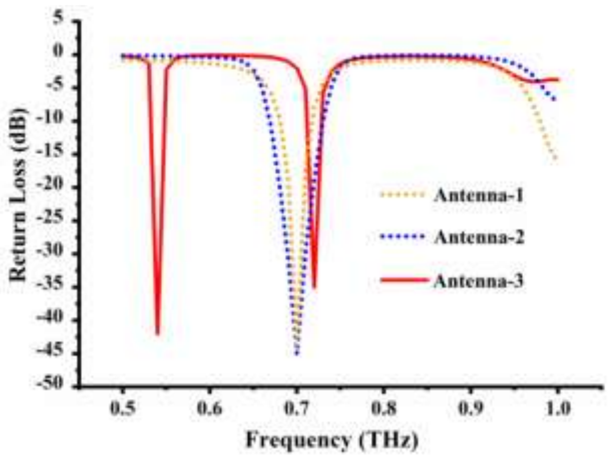

Fig 7. Return Loss Characteristics of Antenna-1, Antenna-2 and Antenna-3

The corresponding Figure 8 and Figure 9 illustrate the gain patterns of Antenna-1 and Antenna-2 at 0.7THz, respectively, and Figure 10 and Figure 11 show the gain distributions of Antenna-3 at its lower and upper resonant frequencies, respectively. The maximum gains increase gradually from 5dB for Antenna-1 to 5.45dB for Antenna-2 and 5.69dB and 6.2dB for lower and upper bands of Antenna-3, respectively. In summary, the figure clearly shows the systematic evolution of the proposed THz antenna from conventional microstrip patch to advanced dual-band DGS-assisted structure, which is evidence of the effectiveness of the synergistic OSRSDGS-HSRSDGS approach for improving impedance matching, bandwidth, resonant behavior and gain in next generation THz communication systems.

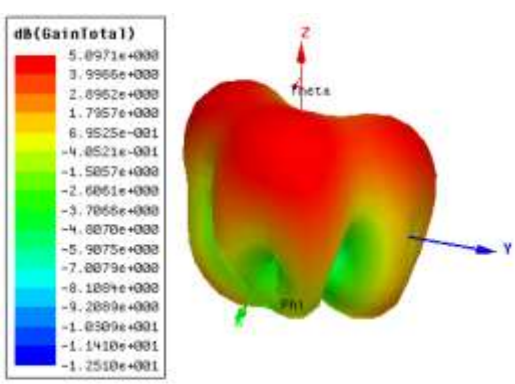

Fig 8. Total Peak Gain of Antenna-1

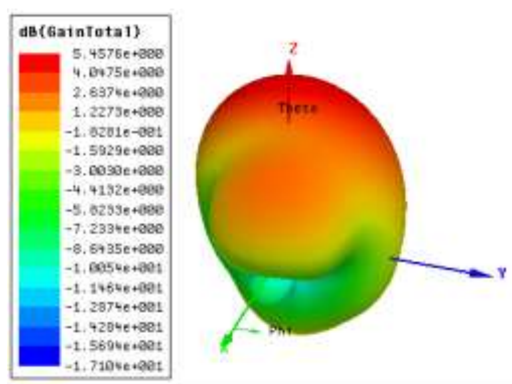

Fig 9. Total Peak Gain of Antenna-2

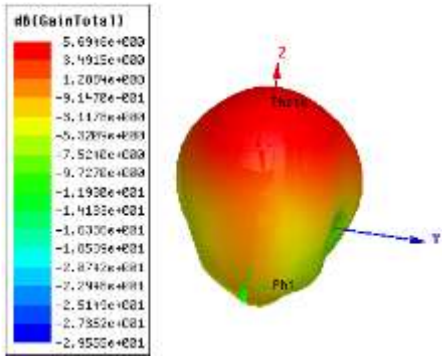

Fig 10. Total Peak Gain of Antenna-3 at 0.55THz

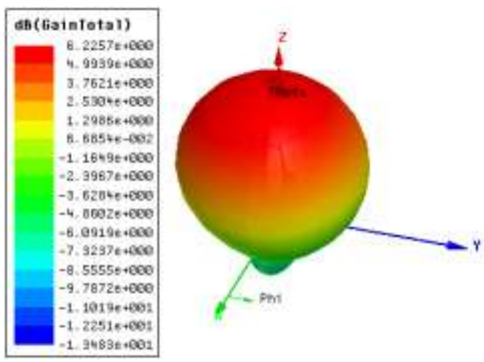

Fig 11. Total Peak Gain of Antenna-1at 0.73THz

The progressive performance improvement achieved by the proposed DGS-based design strategy is summarized in Table 1.

Table 1. Performance Evolution of Proposed Antennas

Parameter	**Antenna-1**	**Antenna-2**	**Antenna-3**	
Resonant Frequency (THz)	0.7	0.7	0.55	0.73
Return Loss (dB)	−35	−40	−43	−34
Bandwidth (GHz)	120	130	47	44
Peak Gain (dB)	5	5.45	5.69	6.2

A based on Antenna-3, two-element Multiple-Input Multiple-Output (MIMO) architecture has been designed for improving the system capacity, spectral efficiency and link reliability in THz communication environment. The MIMO configuration was realized with two identical Antenna-3 elements side-by-side with inter-element spacing of λ/4 (λ is the free-space wavelength at the operating frequency). This spacing was selected to provide an optimum compromise between compactness and separation of elements. The corresponding MIMO configuration is denoted as Antenna-4 and illustrated in Figure 12.

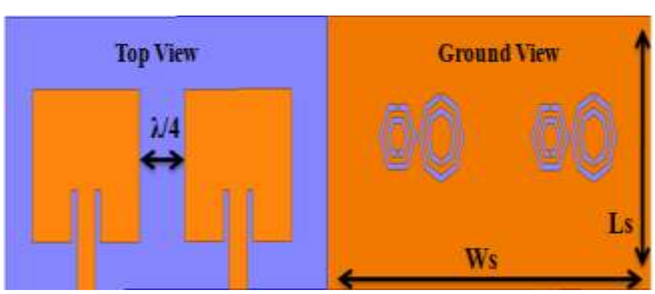

Fig 12. Geometry of Antenna-4

The Antenna-4 design retains the dual band property of the original radiator by employing λ/4 (λ is the free-space wavelength at the operating frequency)-spaced antenna elements. Resonances are observed at 0.55THz and 0.73THz as shown in Figure 13. The simulated return-loss characteristics show the dual band operation at these frequencies for S(1, 1) and S(2, 2). The return losses of S(1, 1) and S(2, 2) responses are around -43dB and -22dB at 0.55THz and -34dB and -45dB at 0.73THz respectively. The corresponding -10dB impedance bandwidths are 47GHz and 44GHz for the lower and upper operating bands respectively. The resonance frequencies of both the reflection coefficients are in good agreement with each other which confirms the effective operation of both the antenna elements and validates the balanced performance of Antenna-4 in the proposed MIMO configuration.

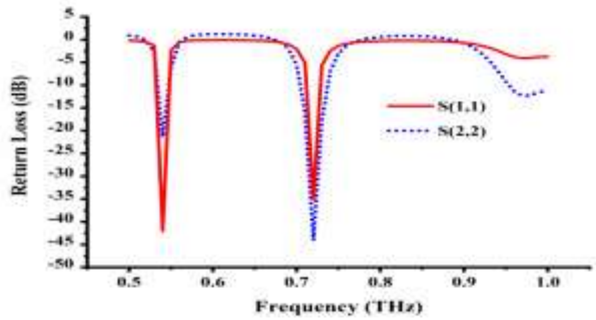

Fig 13. Return Loss Characteristics of Antenna-4

Figures 14 and 15 depict the gain distributions of Antenna-4 at the lower and upper resonant frequencies, respectively. The antenna demonstrates peak gains of 6.40dB and 6.64dB, validating the effectiveness of the proposed DGS-assisted wide-aperture MIMO design. The proposed antenna has improved gain, dual band operation and small size which make it a good candidate for high performance next generation THz wireless communication systems.

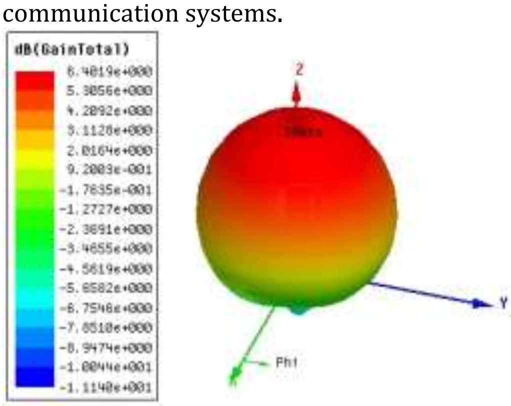

Fig14. Total Peak Gain of Antenna-4 at 0.55THz

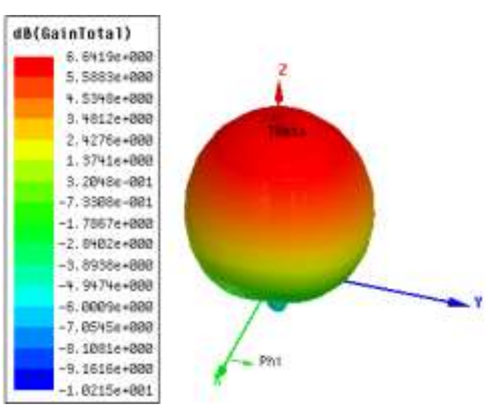

Fig15. Total Peak Gain of Antenna-4 at 0.73THz

The achievable data rate is estimated by Shannon's channel capacity theorem to evaluate the communication performance using equation (5), [34][43] where C is the channel capacity, B is the bandwidth, and S/N is the signal-to-noise ratio (SNR). For the short-range THz communication assuming SNR=20 dB, estimated capacities are 0.80Tbps for Antenna-1 (with 120GHz bandwidth), 0.86Tbps for Antenna-2 (with 130 GHz bandwidth), and 0.31Tbps and 0.29Tbps for the dual-band Antenna-3 at 0.55THz and 0.73THz, respectively, with bandwidths of 47GHz and 44GHz.

$$C = Blog_2\left(1+\frac{S}{N}\right) bits/s/\, H_z \qquad (5)$$

The channel capacity for the two element MIMO antenna (Antenna-4) is calculated using the MIMO capacity expressions (6) and (7), [43].

$$C = Blog_2\left[det\left(I_M + \frac{S}{N}HH^*\right)\right] \qquad (6)$$

Where H is the channel matrix and I_m is an identity matrix.

$$I_M = \begin{bmatrix} 1 & \cdots & 0 \\ \vdots & \ddots & \vdots \\ 0 & \cdots & 1 \end{bmatrix} \quad H = \begin{bmatrix} H_{1,1} & \cdots & H_{1,T} \\ \vdots & \ddots & \vdots \\ H_{R,1} & \cdots & H_{R,T} \end{bmatrix} \qquad (7)$$

The estimated capacities are 0.63Tbps at 0.55THz and 0.59Tbps at 0.73THz, which is almost two times higher than Antenna-3, using spatial multiplexing without increasing the bandwidth or SNR. These results show that MIMO is effective for improving the channel capacity and spectral efficiency for future THz wireless communication systems.

In addition, the MIMO performance of Antenna-4 is investigated using Envelope Correlation Coefficient (ECC). Figure 16 shows that the ECC calculated with Equation (8), [43] is about 0.01 for both the 0.55THz and 0.73THz operating bands, which indicates the very low correlation and good isolation between the antenna elements. The low value of ECC proves the usability of the designed antenna for efficient spatial multiplexing and MIMO operation. A Further, evaluation of the diversity characteristics of Antenna-4 is also analyzed in terms of the Diversity Gain (DG) [34]. The calculated DGs using Equation (9) are 10 dB at the 0.55THz and 0.73THz frequency bands respectively. It is close to the ideal value for the two-element MIMO system as shown in Figure 17. This result confirms the excellent diversity characteristics of the proposed antenna, which improves the link reliability and allows for robust high speed THz communication.

$$\rho = \frac{|S_{11}S_{12} + S_{21}S_{12}|^2}{(1-|S_{11}|^2-|S_{21}|^2)(1-|S_{22}|^2-|S_{12}|^2)} \qquad (8)$$

$$DG = 10\sqrt{1-|\rho|^2} \qquad (9)$$

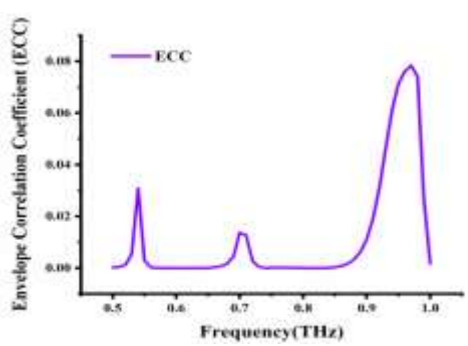

Fig 16. ECC of Antenna-4

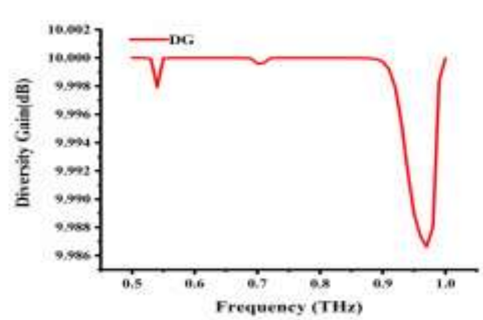

Fig 17. DG of Antenna-4

4. Machine Learning Validation

A full-wave electromagnetic simulation is a powerful technique to analyze terahertz (THz) antennas. However, each change in the antenna geometry requires a new solution of Maxwell's equations. This is computationally involved and requires long simulation times. The problem is even more pronounced in antenna design optimization where thousands of simulations may be required to explore a large design space. To overcome this limitation, we propose a machine learning (ML)-based surrogate modeling framework to establish the mapping from the antenna design parameters to the corresponding electromagnetic responses. The trained ML model can predict the antenna characteristics with high accuracy and speed. This reduces the computing and accelerates the process of design. The HFSS-ML framework for performance prediction and validation of the designed MIMO antenna is shown in Figure 18.

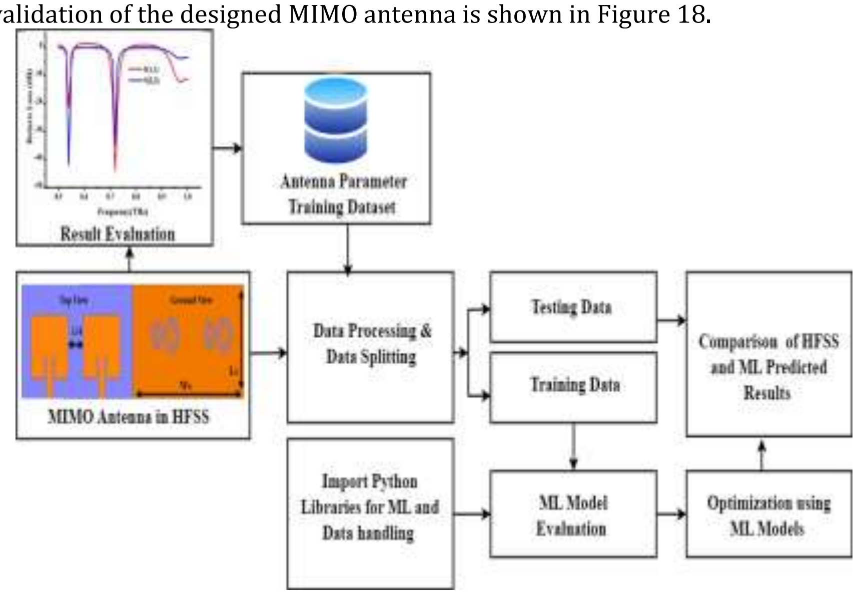

Fig 18. ML Model Training for Antenna-4

The antenna geometry is simulated in HFSS and a detailed parametric study is performed by systematically varying the key design parameters such as antenna dimensions and substrate properties. These simulations provide a data set consisting of 36000 samples. The geometrical and material parameters are the input features and the resonant frequency, bandwidth and scattering parameters of each sample are the corresponding outputs. The generated dataset is pre-processed to ensure data quality and consistency before building the model. This step includes data cleaning, correcting wrong and invalid values, formatting changes, normalization, and feature scaling if needed. The data set is divided into training and testing sets with the ratio 80:20. The relationship between the antenna parameters and the electromagnetic responses is learned from the training dataset. The developed models are tested on the testing dataset to evaluate their generalization ability. In this study, four supervised machine learning algorithms, i.e. Decision Tree (DT), Random Forest (RF), K-Nearest Neighbors (KNN) and XGBoost are explored to model the nonlinear behavior of the antenna system accurately. The algorithms were selected on the basis of their ability to model complex non-linear relationships, handle large data sets, reduce over-fitting and efficiently address multiple input features [44–46]. The models are being developed using Python libraries such as NumPy, Pandas for data processing, Matplotlib for visualization and Scikit learn for machine learning model development. The individual models are used to predict antenna performance parameters and to emulate electromagnetic responses obtained from HFSS simulations after training.

The predictive performance of the developed models is quantitatively evaluated by the Mean Squared Error (MSE), Root Mean Squared Error (RMSE), Mean Absolute Error (MAE) and the coefficient of determination (R^2) presented in equations (10-13) [45-46]. The corresponding error metrics and R^2 performance are presented in Figure 19 and their numerical comparisons are summarized Table.2

$$MSE = \frac{1}{N}\sum_{i=1}^{N}(y_i - \tilde{y_i})^2 \qquad (10)$$

$$RMSE = \sqrt{MSE} \tag{11}$$

$$MAE = \frac{1}{N}\sum_{i=1}^{N}|y_i - y_i^{\sim}| \tag{12}$$

$$R^2 = \frac{\sum_{i=1}^{N}(y_i - y_i^{\sim})^2}{\sum_{i=1}^{N}(y_i - \overline{y}_i)^2} \tag{13}$$

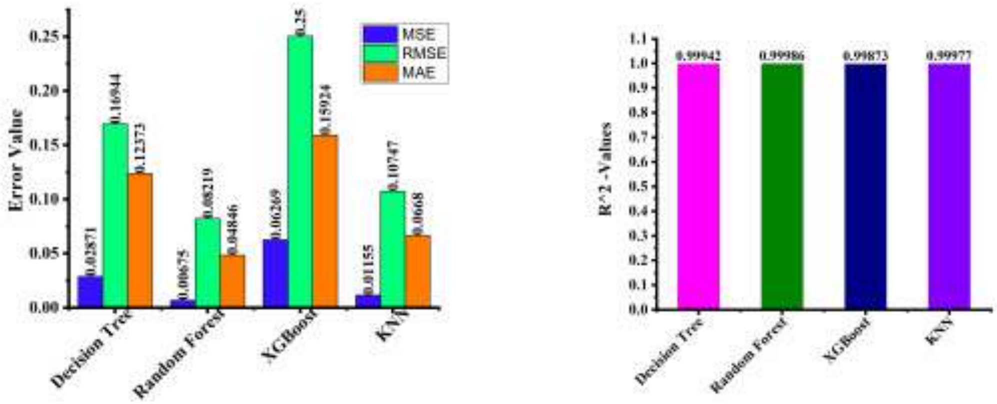

Fig 19. Error Metrics and R^2 Performance of Proposed Machine Learning Models

Table 2. Performance Compression of Machine Learning Models

Model	MSE	RMSE	MAE	R^2
Decision Tree	0.02871	0.16944	0.12373	0.99942
Random Forest	0.00675	0.08219	0.04846	0.99986
XGBoost	0.062669	0.25000	0.15924	0.99873
KNN	0.01155	0.10747	0.06680	0.99977

The evaluation metrics provide a measure of the magnitude of prediction errors and correlation between predicted and simulated responses to give an overall measure of the prediction accuracy. From the observation of Table 2, all ML models the best predictive accuracy among the studied approaches was achieved by the Random Forest model with MSE of 0.00675, RMSE of 0.08219, MAE of 0.04846 and R^2 value of 0.99986. The very low errors and R^2 score near to 1 show the ability of the model to learn and reproduce very well the complex electromagnetic properties of the proposed antenna. We choose the Random Forest model for further validation based on this improved performance. The comparison of the return-loss characteristics of the Random Forest surrogate model and the HFSS simulation results, as shown in Figure 20, verifies the reliability of the surrogate model. The comparison shows a very good agreement of the two approaches in the whole range operation frequencies. HFSS simulation shows dual band resonances at 0.55THz and 0.73THz with good impedance matching properties. The Random Forest model is able to reproduce the resonant frequencies and the related return loss behavior with a good accuracy, following closely the trend and the magnitude of the simulated responses. The slight difference between the curves of the predicted and the simulated values confirms that the trained model has learned the resonance mechanisms and electromagnetic characteristics of the proposed antenna. Good agreement between the results obtained with HFSS and ML validates the proposed surrogate model based on Random Forest. The developed framework allows an accurate and reliable prediction of the antenna performance with a significant reduction of the computational load of repeated full-wave electromagnetic simulations. Therefore, the proposed method is an effective tool for fast analysis and optimization of the antenna and future applications in THz antenna design.

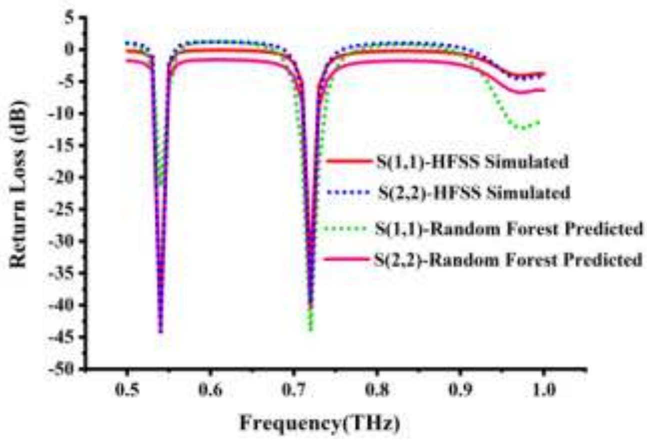

Fig 20. Comparison of Simulated and RFML Predicted Return Loss Characteristics for Antenna-4

5. RLC Model Validation Using MATLAB

Full-wave electromagnetic simulation is a reliable method for studying THz antennas. However, any change of the antenna geometry requires re-solving of the Maxwell's equations, which leads to high computational cost and long simulation time. Antenna optimization and the analysis of a large number of design parameters often require many thousands of simulations. To overcome this limitation, the relation between the antenna design parameters and electromagnetic responses is modeled with the aid of machine learning (ML) as a surrogate modeling approach from the simulation data. The trained ML model can predict the antenna characteristics with high accuracy and short time after training, which greatly reduces the computation work and allows efficient antenna design and optimization. The proposed THz MIMO antenna was validated using an equivalent lossy series RLC circuit model in MATLAB in addition to the HFSS full-wave simulation and Random Forest based Machine Learning (RFML). The circuit parameters were calculated by using (14)–(18) [37] from the simulated resonant frequencies and related bandwidths. The first resonance at 0.55THz has a bandwidth of 47GHz and an input resistance of about 50Ω. The extracted parameters are Q1=11.70, C1=0.495fF, L1=169.3pH, 50Ω and Γ1 =0. The calculated parameters for the second resonance of 0.73THz with bandwidth of 44GHz are Q2 = 16.59, C2 = 2.63 × 10−16F, L 2 = 1.81 × 10−10H, Z2 = 50 Ω and Γ2 = 0. These extracted parameters reproduced the antenna characteristics by the equivalent RLC circuit model.

$$Q = \frac{f_r}{BW} \quad (14)$$

$$C = \frac{1}{2\pi f_r RQ} \quad (15)$$

$$L = \frac{QR}{2\pi f_r} \quad (16)$$

$$Z(\omega) = 60 + j\left(\omega L - \frac{1}{\omega C}\right) \quad (17)$$

$$\Gamma = \frac{Z-50}{Z+50} \quad (18)$$

The corresponding RLC model shows the resonances at 0.55THz and 0.73THz with the S_{11} return loss values of about -43dB and -34dB respectively. Also, the S_{22} response as shown in Figure 21 demonstrates the return loss values of about −22dB at 0.55THz and −45dB at 0.73 THz with the bandwidths of 47GHz and 44GHz. The return loss characteristics of the equivalent RLC circuit model, HFSS simulation and RFML prediction are compared and excellent agreement is observed for resonant frequencies, return loss and bandwidth. This close correlation confirms the RFML model can provide fast and accurate antenna performance prediction with much lower computational cost. The equivalent RLC model on the other hand provides a physically meaningful approach to the antenna resonance mechanism with the circuit parameters. The good agreement of HFSS, RFML and RLC results from validates the proposed THz MIMO antenna design and provides an efficient framework for antenna analysis, fast performance prediction and future design optimization.

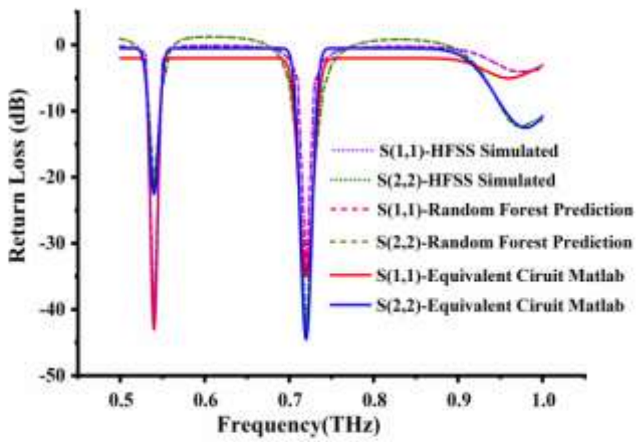

Fig 21. Comparison of HFSS Simulation, RFML Prediction, and RLC Model Responses for Antenna-4

Furthermore, the combination of the HSRSDGS and OSRSDGS unit cells leads to a considerable virtual size reduction (VSR) of the designed antenna. The VSR is given by (19).

$$VSR = \left(\frac{L_1 - L_2}{L_1}\right) * 100 \qquad (19)$$

Here, L1 is the patch length of the lower-band resonance of Antenna-4 (0.55 THz) and L2 is the patch length of the conventional reference antenna (Antenna-1). The lower-frequency resonance is mainly contributed by the HSRSDGS that increases the effective current path, while the higher-frequency resonance is mainly contributed by the OSRSDGS. Thus, Antenna-4 has a 21.26% virtual size reduction. It shows that the proposed antenna resonates at 0.55THz but it has much more compact size than a conventional antenna at the same operating frequency. The proposed Antenna main results are summarized in Table 3.

Table 3. Performance Evolution of Proposed Antennas

Antenna Type	Resonate Frequency (THz)	Bandwidth (GHz)	Data Rate (Tbps)	Gain (dB)	ECC	DG (dB)	VSR (%)	ML Model	RLC Model
[7]	0.7	85	0.56	3.5	-	-	-	✗	✗
[8]	0.95	109	0.72	5.46	-	-	-	✗	✗
[9]	0.7	100	0.66	5.9	-	-	-	✗	✗
[10]	0.65	69	0.91	8	0.028	9.98	-	✗	✗
[11]	30	69.6	0.92	7.6	0.01	10	-	✗	✗
[12]	30	83	0.42	10.3	-	-	-	✗	✗
[13]	1.8	170	0.55	7.1	-	-	-	✗	✗
[14]	38	64	0.59	14.2	-	-	-	✗	✗
[15]	28	90	1.13	6.8	-	-	-	✗	✗
[25]	0.4	87	1.15	5	0.042	9.97	-		✗
[26]	0.45	98	1.30	6.9	0.2	9.7	-		✗
[27]	0.6	102	1.35	5.7	0.125	9.92	-		✗
[31]	0.7	108	1.43	6.5	0.23	9.73	-		✗
[38]	0.7	110	1.46	5.9	0.09	9.96	-		✗

[39]	0.7		112		1.49		5.4		0.185	9.83	-		✗
Antenna-1	0.7		120		0.80		5.09		-	-	-	✗	✗
Antenna-2	0.7		130		0.86		5.45		-	-	-	✗	✗
Antenna-3	0.55	0.73	47	44	0.31	0.29	5.69	6.22	-	-	-		
Antenna-4	0.55	0.73	47	44	0.63	0.59	6.40	6.64	0.01	10	21.3		

6. Conclusion

In this paper, a multidisciplinary framework integrating THz MIMO antenna design with machine learning and equivalent circuit modeling is proposed for a complete antenna analysis and validation. A two element THz MIMO antenna based on hybrid OSRSDGS-HSRSDGS configuration is designed and investigated. The suggested antenna demonstrates its suitability for high-performance THz MIMO applications with dual-band stability at 0.55THz and 0.73THz, featuring return losses approximately -43dB and -34dB, bandwidths of 47GHz and 44GHz, peak gains of 6.4dB and 6.6dB, ECC of 0.01 and diversity gain of 10dB. Further improvement of the design methodology was achieved by machine learning techniques using datasets generated from HFSS simulations. Among the models evaluated (DT, RF, KNN and XGBoost), the Random Forest algorithm had the highest accuracy in prediction with R^2 value of 0.99 and low error metrics (MSE = 0.00675, RMSE = 0.08219 and MAE = 0.04846), demonstrating its ability to accurately predict the performance of the antenna with significant reduction in computational effort. Furthermore, the developed lossy series RLC equivalent circuit model in MATLAB was able to reproduce the antenna resonance and bandwidth characteristics, which validates the electromagnetic behavior at the circuit level. The proposed antenna also exhibits a virtual size reduction of 21.26% suggesting the achievement of the lower-band resonance at 0.55THz with a significantly more compact physical structure than a conventional antenna designed for the same operating frequency. The close agreement between full-wave electromagnetic simulations, machine learning predictions and equivalent circuit analysis confirms the accuracy and reliability of the proposed methodology. The proposed multidisciplinary framework provides an efficient and reliable approach for the design, analysis and validation of compact THz MIMO antennas and can be used as a promising basis for future high frequency wireless communication systems.

Funding

No”.

Conflicts of Interest

The authors declare that they have no conflicts of interest to report regarding the present study.

Acknowledgement

The authors would like to express their sincere gratitude to Lincoln University College, Selangor, Malaysia, and Vignan Institute of Technology and Science, Hyderabad, Telangana, India, for their continuous support and encouragement in carrying out this research work.

I. References

1. Shafie, A., Yang, N., Han, C., Jornet, J. M., Juntti, M., and Kürner, T. (2023). Terahertz communications for 6G and beyond wireless networks: Challenges, key advancements, and opportunities. IEEE Network, 37(3), 162–169. https://doi.org/10.1109/MNET.118.2200057
2. Akyildiz, I. F., Han, C., Hu, Z., Nie, S., and Jornet, J. M. (2022). Terahertz band communication: An old problem revisited and research directions for the next decade. IEEE Transactions on Communications, 70(6), 4250–4285. https://doi.org/10.1109/TCOMM.2022.3171800
3. Jiang, W., Zhou, Q., He, J., Habibi, M. A., Melnyk, S., El-Absi, M., Han, B., Di Renzo, M., Schotten, H. D., Luo, F.-L., El-Bawab, T. S., Juntti, M., Debbah, M., and Leung, V. C. M. (2024). Terahertz communications and sensing for 6G and beyond: A comprehensive review. IEEE Communications Surveys & Tutorials,

26(4), 2326–2381. https://doi.org/10.1109/COMST.2024.3385908
4. Akyildiz, I. F., Jornet, J. M., and Han, C. (2014). Terahertz band: Next frontier for wireless communications. Physical Communication, 12, 16–32. https://doi.org/10.1016/j.phycom.2014.01.006
5. Siegel, P. H. (2002). Terahertz technology. IEEE Transactions on Microwave Theory and Techniques, 50(3), 910–928. https://doi.org/10.1109/22.989974
6. Tonouchi, M. (2007). Cutting-edge terahertz technology. Nature Photonics, 1(2), 97–105. https://doi.org/10.1038/nphoton.2007.3
7. Mittleman, D. M. (2017). Perspective: Terahertz science and technology. Journal of Applied Physics, 122(23), 230901. https://doi.org/10.1063/1.5007683
8. Elayan, H., Amin, O., Shihada, B., Shubair, R. M., and Alouini, M.-S. (2019). Terahertz band: The last piece of RF spectrum puzzle for communication systems. IEEE Open Journal of the Communications Society, 1, 1–32. https://doi.org/10.1109/OJCOMS.2019.2953633
9. Ali, S., Sohail, M., Shah, S. B. H., et al. (2021). New trends and advancement in next generation mobile wireless communication (6G): A survey. Wireless Communications and Mobile Computing, 2021, 9614520. https://doi.org/10.1155/2021/9614520
10. Armghan, A., Aliqab, K., Alsharari, M., Alsalman, O., Parmar, J., and Patel, S. K. (2023). Design and development of ultrabroadband, high-gain, and high-isolation THz MIMO antenna with a complementary split-ring resonator metamaterial. Micromachines, 14(7), 1328. https://doi.org/10.3390/mi14071328
11. Pant, R., and Malviya, L. (2024). Terahertz MIMO antenna array for future generation of wireless applications. Frequenz, 78(5–6), 271–280. https://doi.org/10.1515/freq-2023-0203
12. Saxena, G., Alam, M., Roy, M., Barnawi, A. B., Khan, T. M. Y., Yadava, R. L., Chintakindi, S., Jain, R., Singh, H., and Awasthi, Y. K. (2023). CSRR loaded multiband THz MIMO antenna for nano-communications and bio-sensing applications. Nano Communication Networks, 38, 100481. https://doi.org/10.1016/j.nancom.2023.100481
13. Shiddanagouda, F. B., Aithal, P. S., Nali, D. K., and Lenin Kumar, M. (2024). Designing a millimeter-wave MIMO antenna for sustainable development in 5G technology. In M. A. Alam, F. Siddiqui, S. Zafar, and I. Hussain (Eds.), Proceedings of the 4th International Conference on ICT for Digital, Smart, and Sustainable Development (ICIDSSD 2024). Innovations in Sustainable Technologies and Computing. Springer, Singapore. https://doi.org/10.1007/978-981-97-7831-7_36
14. Saxena, G., et al. (2022). Metasurface inspired wideband high isolation THz MIMO antenna for nano communication including 6G applications and liquid sensors. Nano Communication Networks, 34, 100421. https://doi.org/10.1016/j.nancom.2022.100421
15. Singh, R., and Varshney, G. (2023). Isolation enhancement technique in a dual-band THz MIMO antenna with single radiator. Optical and Quantum Electronics, 55, 539. https://doi.org/10.1007/s11082-023-04811-y
16. Saxena, G., et al. (2024). A quad-port triple-band high isolation terahertz MIMO antenna for short-distance THz communication links. e-Prime—Advances in Electrical Engineering, Electronics and Energy, 9, 100686. https://doi.org/10.1016/j.prime.2024.100686
17. Arya, A. K., Kartikeyan, M. V., and Patnaik, A. (2010). Defected ground structure in the perspective of microstrip antennas: A review. Frequenz, 64(5–6), 79–84. https://doi.org/10.1515/FREQ.2010.64.5-6.79
18. Khandelwal, M. K., Kanaujia, B. K., and Kumar, S. (2017). Defected ground structure: Fundamentals, analysis, and applications in modern wireless trends. International Journal of Antennas and Propagation, 2017, 2018527. https://doi.org/10.1155/2017/2018527
19. Hong, J. S., and Karyamapudi, B. M. (2005). A general circuit model for defected ground structures in planar transmission lines. IEEE Microwave and Wireless Components Letters, 15(10), 706–708. https://doi.org/10.1109/LMWC.2005.856832
20. Kumar, A., and Machavaram, K. V. (2013). Microstrip filter with defected ground structure: A close perspective. International Journal of Microwave and Wireless Technologies, 5(5), 589–602. https://doi.org/10.1017/S1759078713000639
21. Marotkar, D. S., and Zade, P. (2016). Bandwidth enhancement of microstrip patch antenna using defected ground structure. In 2016 International Conference on Electrical, Electronics, and Optimization Techniques, 7754978. https://doi.org/10.1109/ICEEOT.2016.7754978
22. Liu, Y., Yang, X., Jia, Y., and Guo, Y. J. (2019). A low correlation and mutual coupling MIMO antenna.

IEEE Access, 7, 127384–127392. https://doi.org/10.1109/ACCESS.2019.2939270
23. Niu, Z., Zhang, H., Chen, Q., and Zhong, T. (2019). Isolation enhancement for 1 × 3 closely spaced E-plane patch antenna array using defect ground structure and metal-vias. IEEE Access, 7, 119375–119383. https://doi.org/10.1109/ACCESS.2019.2937385
24. Tang, Z., Wu, X., Zhan, J., et al. (2019). Compact UWB-MIMO antenna with high isolation and triple band-notched characteristics. IEEE Access, 7, 19856–19865. https://doi.org/10.1109/ACCESS.2019.2897170
25. Fritz-Andrade, E., et al. (2020). Characteristic mode analysis applied to reduce the mutual coupling of a four-element patch MIMO antenna using a defected ground structure. IET Microwaves, Antennas & Propagation, 14(2), 215–226. https://doi.org/10.1049/iet-map.2019.0570
26. Shiddanagouda, F. B., Aithal, P. S., Srinivasa Reddy, A., Thota, S., and Dinesh Kumar, N. (2024). Design and optimization of dual band millimeter wave MIMO antenna for next generation 5G/6G wireless systems. Journal of Harbin Engineering University, 45(11), 373–380. https://harbinengineeringjournal.com/index.php/journal/article/download/3729/2183/5952
27. Jilani, S. F., and Alomainy, A. (2018). Millimetre-wave T-shaped MIMO antenna with defected ground structures for 5G cellular networks. IET Microwaves, Antennas & Propagation, 12(5), 672–677. https://doi.org/10.1049/iet-map.2017.0467
28. Khalid, M., Naqvi, S. I., Hussain, N., Rahman, M., Mirjavadi, S. S., Khan, M. J., and Amin, Y. (2020). 4-port MIMO antenna with defected ground structure for 5G millimeter wave applications. Electronics, 9(1), 71. https://doi.org/10.3390/electronics9010071
29. Nguyen, N. L. (2019). Gain enhancement in MIMO antennas using defected ground structure. Progress in Electromagnetics Research M, 87, 127–136. https://doi.org/10.2528/PIERM19091102
30. Kumar, P., Pathan, S., Kumar, O. P., Vincent, S., Nanjappa, Y., Kumar, P., Shetty, P., and Ali, T. (2022). Design of a six-port compact UWB MIMO antenna with a distinctive DGS for improved isolation. IEEE Access, 10, 112964–112974. https://doi.org/10.1109/ACCESS.2022.3216889
31. El Misilmani, H. M., and Trinchero, R. (2020). A review on the design and optimization of antennas using machine learning algorithms and techniques. International Journal of RF and Microwave Computer-Aided Engineering, 30(10), e22356. https://doi.org/10.1002/mmce.22356
32. Shiddanagouda, F. B., Vani, R. M., and Hunagund, P. V. (2020). Miniaturized dual-band printed MIMO antenna with DGS for L-band and C-band wireless applications. 2020 IEEE International Conference on Communication, Networks and Satellite (Comnetsat), Batam, Indonesia, 111–116. https://doi.org/10.1109/Comnetsat50391.2020.9328996
33. Khan, M. M., Hossain, S., Mozumdar, P., Akter, S., and others. (2022). A review on machine learning and deep learning for various antenna design applications. Heliyon, 8(4), e09317. https://doi.org/10.1016/j.heliyon.2022.e09317
34. Sarker, N., Podder, P., Mondal, M. R. H., Shafin, S. S., and Kamruzzaman, J. (2023). Applications of machine learning and deep learning in antenna design, optimization, and selection: A review. IEEE Access, 11, 103890–103915. https://doi.org/10.1109/ACCESS.2023.3317371
35. Sharma, Y., Zhang, H. H., and Xin, H. (2020). Machine learning techniques for optimizing design of double T-shaped monopole antenna. IEEE Transactions on Antennas and Propagation, 68(7), 5658–5663. https://doi.org/10.1109/TAP.2020.2966051
36. Cui, L., Zhang, Y., Zhang, R., and Liu, Q. H. (2020). A modified efficient KNN method for antenna optimization and design. IEEE Transactions on Antennas and Propagation, 68(10), 6858–6866. https://doi.org/10.1109/TAP.2020.3001743
37. Li, W. T., Tang, H. S., Cui, C., Hei, Y. Q., and Shi, X. W. (2022). Efficient online data-driven enhanced-XGBoost method for antenna optimization. IEEE Transactions on Antennas and Propagation, 70(7), 4953–4964. https://doi.org/10.1109/TAP.2022.3157895
38. Wu, Q., Chen, W., Yu, C., Wang, H., and Hong, W. (2024). Machine-learning-assisted optimization for antenna geometry design. IEEE Transactions on Antennas and Propagation, 72(3), 2083–2095. https://doi.org/10.1109/TAP.2023.3346493
39. Gupta, A., Karahan, E. A., Bhat, C., Sengupta, K., and Khankhoje, U. K. (2023). Tandem neural network based design of multiband antennas. IEEE Transactions on Antennas and Propagation, 71(8), 6308–6317. https://doi.org/10.1109/TAP.2023.3276524
40. Khan, M. R., Zekios, C. L., Bhardwaj, S., and Georgakopoulos, S. V. (2024). A deep learning convolutional neural network for antenna near-field prediction and surrogate modeling. IEEE Access, 12, 39737–

39747. https://doi.org/10.1109/ACCESS.2024.3377219

41. Koziel, S., Calik, N., Mahouti, P., and Belen, M. A. (2022). Accurate modeling of antenna structures by means of domain confinement and pyramidal deep neural networks. IEEE Transactions on Antennas and Propagation, 70(3), 2174–2188. https://doi.org/10.1109/TAP.2021.3111299
42. Wu, Q., Chen, W., Yu, C., Wang, H., and Hong, W. (2021). Multilayer machine learning-assisted optimization-based robust design and its applications to antennas and arrays. IEEE Transactions on Antennas and Propagation, 69(9), 6052–6057. https://doi.org/10.1109/TAP.2021.3069491
43. Haack, M. P., Jenkins, R. P., Mai, W., Mackertich-Sengerdy, G., Campbell, S. D., Pantoja, M. F., and Werner, D. H. (2024). Physically realizable antenna equivalent circuit generation. IEEE Access, 12, 33652–33658. https://doi.org/10.1109/ACCESS.2024.3370030
44. Huang, Y., Alieldin, A., and Song, C. (2021). Equivalent circuits and analysis of a generalized antenna system. IEEE Antennas and Propagation Magazine, 63(2), 53–62. https://doi.org/10.1109/MAP.2021.3053976
45. Costa, F., Monorchio, A., and Manara, G. (2014). An overview of equivalent circuit modeling techniques for frequency selective surfaces and metamaterials. Applied Computational Electromagnetics Society Journal, 29(12), 960–976. https://doi.org/10.1109/MAP.2014.7019855
46. Katapaka Yadaiah, Jillella Venkateswara Rao, Sivangi Ravikanth, S. Venkata Achuta Rao, K. V. Ganesh, and K. Prem Sagar. (2026). Optimized hybrid precoding in mmWave massive MIMO via federated reinforcement learning and metaheuristic swarm optimization. International Journal of Computer Information Systems and Industrial Management Applications, 18(3s), 1–11. https://doi.org/10.70917/ijcisim-2026-227
47. Jillella Venkateswara Rao, Pydimarri Padmaja, Sivangi Ravikanth, Katapaka Yadaiah, K. V. Ganesh, and M. Khaleel Ullah Khan. (2026). Mobility-robust beamforming for multi-cell integrated sensing and communication using temporal federated learning. Journal of Intelligent Decision Making and Information Science, 3(6s), 180–192. https://doi.org/10.59543/jidmis.v3.1386